Adaptive virus detection using filament-coupled antibodies

Gregory P. Stone
Kelvin S. Lin
Frederick R. Haselton
Vanderbilt University
Biomedical Engineering
Nashville, Tennessee 37235
E-mail: rick.haselton@vanderbilt.edu

Abstract. We recently reported the development of a filament-antibody recognition assay (FARA), in which the presence of virions in solution initiates the formation of enzyme-linked immunosorbent assay (ELISA)-like antibody complexes. The unique features of this assay are that processing is achieved by motion of a filament and that, in the presence of a virus, antibody-virus complexes are coupled to the filament at known locations. In this work, we combine the unique features of this assay with a 638-nm laser-based optical detector to enable adaptive control of virus detection. Integration of on-line fluorescence detection yields approximately a five-fold increase in signal-to-noise ratio (SNR) compared to the fluorescence detection method reported previously. A one-minute incubation with an M13K07 test virus is required to detect 10^{10} virions/ml, and 40 min was required to detect 10^8 virions/ml. In tests of the components of an adaptive strategy, a 30-min virus (3.3×10^{10} virions/ml) incubation time, followed by repositioning the filament-captured virus either within the detecting antibody chamber, $(20 \mu g/ml)$ or within the virus chamber, found an increase in signal roughly proportional to the cumulative residence times in these chambers. Furthermore, cumulative fluorescence signals observed for a filament-captured virus after repeated positioning of the filament within the virus chamber are similar to those observed for a single long incubation time. The unique features of the FARA-like design combined with online optical detection to direct subsequent bioprocessing steps provides new flexibility for developing adaptive molecular recognition assays. © *2006 Society of Photo-Optical Instrumentation Engineers.* [DOI: 10.1117/1.2209907]

Keywords: virus detection; antibody recognition; filament coupling; fluorescence detection.

Paper 05361R received Dec. 1, 2005; revised manuscript received Mar. 10, 2006; accepted for publication Mar. 13, 2006; published online Jun. 6, 2006.

1 Introduction

The need for fast, reliable pathogen detection is increasing, due in part to a better understanding of the role of pathogens in disease and to the rising threat of bioterrorism. Traditional methods using existing laboratory infrastructure and equipment are still the most reliable and robust techniques and can be used to detect a broad range of pathogens. However, most of these techniques require highly trained laboratory personnel and can be both labor and time intensive. Since these methods typically involve growth of the organism in culture or infection of a virus in a suitable host, these techniques may also require days before identification of the pathogen is complete.[1,2]

Many immunological methods have been developed that encompass a broad range of applications such as the detection of bacterial cells, spores, viruses, proteins, or any other toxin that elicits an immune response.[1–3] Numerous new immunological detection strategies have been reported in the litera-

ture, and several reviews have been written summarizing the state of the art of immunological biosensors.[1,4,5] Several of these methods are based on changes in electrical properties as antigen binds to an antibody-coated substrate.[5–9] Many others have been reported that incorporate optical detection of bound antigen. For example, evanescent waves have been used to excite bound antigen on a fiber optic waveguide using a fluorescently labeled detecting antibody.[10] Rowe et al. and Ligler et al. have extended this technique to incorporate a 2-D waveguide which an entire array of probe molecules has been immobilized.[11,12] However, many of these assays require complex microfluidics, and automation of fluid handling and processing is very difficult to incorporate into these systems. In addition, these optical techniques usually do not incorporate a feedback mechanism to determine when the detection signal has reached an adequate level. Therefore, test parameters are conservatively set by the assay conditions necessary to detect the minimum concentration of pathogen.

We have recently reported the development of a filament-antibody recognition assay (FARA), which appears to poten-

Address all correspondence to Rick Haselton, Biomedical Engineering, Vanderbilt University, VU Station B - Box 351631 Nashville, TN 37235; Tel: 615-322-6622; Fax: 615-343-7919; E-mail: rick.haselton@vanderbilt.edu
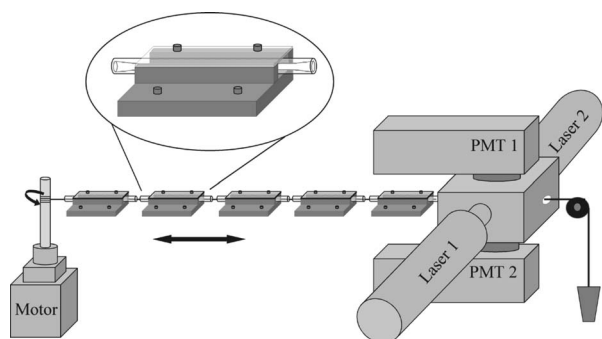
Fig. 1 Assay design schematic. Filament-coupled capture antibodies are positioned within a series of five reaction chambers before passing through a fluorescence detector. Filament associated virus is detected fluorescently using diode laser excitation and photomultipliers.

tially have much greater flexibility.[13] We now report the integration of an on-line optical detection method to enable adaptive feedback control of virus detection. Briefly, FARA is a sandwich-based immunoassay in which virus capture antibodies are immobilized on the surface of a monofilament rather than on a polystyrene plate in typical enzyme-linked immunosorbent assay (ELISA). Using a rotary stage to control filament position, each capture antibody region of the filament is passed through a series of five reaction chambers containing virus test solution and the immunoassay processing solutions (Fig. 1). In this work, the capture antibody regions on the filament are then passed through an integrated detector and examined for the presence of fluorescently labeled detecting antibody. In theory, fluorescence values could be used to determine if virus is present in the test solution, or if further processing and additional testing is required. For example, an initial rapid test that is negative might be followed up by a slower test with greater sensitivity. The experimental results reported here suggest that this feedback design provides additional flexibility in the immunoassay design and makes adaptive detection feasible.

2 Materials and Methods

2.1 Antibody and Virus Reagents

M13K07 phage and anti-M13 monoclonal antibody were used as a model system for this study. M13K07 is well characterized and can be handled with minimal safety concerns. M13K07 virus (M13) was obtained from the Vanderbilt Molecular Recognition and Screening facility (Nashville, Tennessee) in a stock concentration of 3.3×10^{11} virions/ml, and was diluted in phosphate buffered saline (PBS) containing 0.1% tween-20 (PBS-T) to working concentrations immediately prior to the experiments. Anti-M13 monoclonal IgG_{2a} (anti-M13) and anti-E tag monoclonal IgG_{2a} (anti-E) were obtained from Amersham Biosciences (Piscataway, New Jersey). Anti-M13 was used both as a capture antibody and a detecting antibody as described later. Anti-E was used as a nonspecific control for virus capture. Anti-M13 detecting antibody was made by fluorescently labeling anti-M13 antibody with Alexa Fluor 647 (AF647, Molecular Probes, Eugene, Oregon). Labeling procedures were performed according to the manufacturers' instructions. The concentration of the labeled

antibody along with the degree of labeling was calculated from the absorbance at 280 nm (IgG molar extinction coefficient: $213,000 \text{ cm}^{-1}\text{M}^{-1}$) and the peak label absorbance (650 nm, $239,000 \text{ cm}^{-1}\text{M}^{-1}$). Working solutions of both labeled and unlabeled antibody were stored at $4 °C$, and for long-term storage aliquots were stored at $-20 °C$.

2.2 Antibody Immobilization on Filament

Unlabeled anti-M13 and anti-E capture antibodies were passively adsorbed to a clear polyester monofilament with a diameter of 120 μm (Sulky Invisible, Punta Gorda, Florida). This monofilament was selected because of its low autofluorescence properties and its nonporous surface. This latter property permits rapid processing while avoiding filament swelling. The monofilament was wound around the ends of a PhastGel sample applicator (Amersham Biosciences) and placed within the concave teeth as described previously.[13] The comb/filament apparatus was washed in 70% ethanol, rinsed in water, washed in 10% HCl, and rinsed again. The filament was dried and 0.75 μl of capture antibody solution (500 μg/ml) was pipetted onto each tooth of the comb. The comb and filament were incubated in a humidified box for 45 min to allow time for adequate adsorption of the capture antibody to the filament. Following incubation, the comb and filament were rinsed in PBS-T to remove unbound capture antibody from the filament. Filaments were used within one hour of the final rinse.

2.3 Filament Processing

One-quarter-inch (OD) thick-walled glass capillary tubing with either 2-mm ID or 0.75-mm ID was cut into 75 mm lengths, and the ends were flared outward to facilitate smooth movement of the filament through the chambers. Table 1 summarizes the dimensions, contents, and function of each chamber. Chamber solutions were loaded manually using a pipette. Each glass chamber was housed in an aluminum holder with holes for two positioning bolts, as shown in the inset of Fig. 1. A horizontal aluminum stage with a matrix of predrilled holes was used to align the chambers. The spacing between chambers was approximately 1 cm. After a filament was threaded through the chambers and detector, it was attached to a rotating spindle atop the rotary stage. A small weight on the opposite end kept the filament under low tension and centered within the middle of each chamber (Fig. 1).

Filament movement through the five chambers and detector was performed using a rotary stage and control system (Sigma II Servo System, Yaskawa, Waukegan, Illinois). The rotary stage was controlled through a LabView Virtual Instrument (National Instruments, Austin, Texas) that positioned the filament regions containing capture antibody within each chamber. The LabView interface controlled the speed of the filament through the chambers, oscillatory movements within the chambers, and the total residence time within each chamber. Overall distance from the first chamber through the detector was approximately 50 cm.

2.4 Fluorescence Detection

After bioprocessing, a laser excitation source was used to excite the fluorescently labeled detecting antibody associated with antibody-virus complexes on the filament. The detection

Table 1 Contents and description of each chamber.

Chamber	ID/volume (mm/μl)	Solution	Function
1	2/235	PBS-T	Rehydrate probes, block nonspecific binding
2	0.75/60	M13 virus	Expose immobilized antibody to antigen
3	2/235	PBS-T	Wash away unbound antigen
4	0.75/60	Labeled anti-M13 antibody	Expose bound virus to labeled antibody
5	2/235	PBS-T	Wash away unbound labeled antibody

system incorporated two diode lasers at a 90-deg orientation to the filament. The dual laser design allowed for flexibility when choosing appropriate fluorescent labels for detection. The filament was threaded through a detection chamber (Newport-Oriel, Stratford, Connecticut) that allowed easy coupling of two lasers and two photomultiplier tubes (PMT). Figure 1 shows a diagram of the virus detection scheme and its position relative to the bioprocessing chambers. Laser 1 (638-nm, 25-mW diode laser, Coherent, Santa Clara, California) was used to excite the AF647 fluorescent dye. Laser 2 (532-nm, 20-mW diode-pumped, solid state laser, B&W Tek, Incorporated, Newark, Delaware) was used to excite AF555 fluorescent dye, which was used primarily in preliminary experiments. The detector's dual laser and dual PMT design permits two fluorescent labels to be used concurrently, adding flexibility to this technique. The lasers were attached to the detection chamber on either side using custom adaptors to fit the ports of the detection chamber. A polarizer was placed within the adaptor to reduce the 638-nm laser power to approximately 5 mW.

The PMTs were also attached via custom adaptors to the top and bottom of the chamber. Reflectance of the laser light from the filament was a significant source of noise, so the choice of emission filters was critical to achieving a high signal to noise ratio (SNR). For the AF647 channel, long-pass filters with cutoffs at 685 nm (Chroma, Rockingham, Verment) and 665 nm (Melles Griot, Rochester, New York) were combined to filter out reflected laser light. The AF555 channel combined a bandpass filter centered at 565 nm (30-nm bandwidth, Chroma) with a long-pass filter (570-nm cutoff, Melles Griot) to filter out reflected light. Filters were placed between the sample chamber and the PMTs as shown in Fig. 2.

Figure 2 shows the optical path for the detector. A custom brass slit ($\sim$1 mm wide) was placed in the laser path to minimize the area on the filament illuminated by the laser. After exciting bound detecting antibody, fluorescence emission from the detecting antibody passed through a pinhole that reduced much of the reflected laser light. The light then passed through a pair of emission filters, which removed reflected excitation light while allowing emitted light to pass through to the PMT (R928, Hamamatsu). Each PMT was powered by an 800-V signal (Pacific Instruments, Concord, California), and the resulting current was converted to voltage and amplified by a factor of 10^5 by a transimpedance ampli-

fier (Model 101C, UDT Instruments, Baltimore, Maryland). The amplified voltage (0 to 14 V) was sampled by a digital acquisition board (BNC 2120, National Instruments) controlled through a LabView virtual instrument. Filament movement and signal sampling were synchronized using a single LabView interface.

2.5 Experimental Parameters

Filament movement parameters were held constant throughout all experiments. Filament speed between chambers was maintained at 2 cm/s, and filament regions were oscillated a distance of 2 cm at 1 cm/s within each chamber for the requisite length of time. All filaments were blocked in chamber 1 for 15 min before experiments were started. All experiments used M13K07 virus (3.3×10^{10} virions/ml, unless otherwise noted) and used AF647 anti-M13 (20 mg/ml) for detection. Other bioprocessing components were the same in all experiments. SNR was defined as the average peak height of anti-M13 regions divided by the peak height of a negative control anti-E region. An unpaired t-test was used to compare average
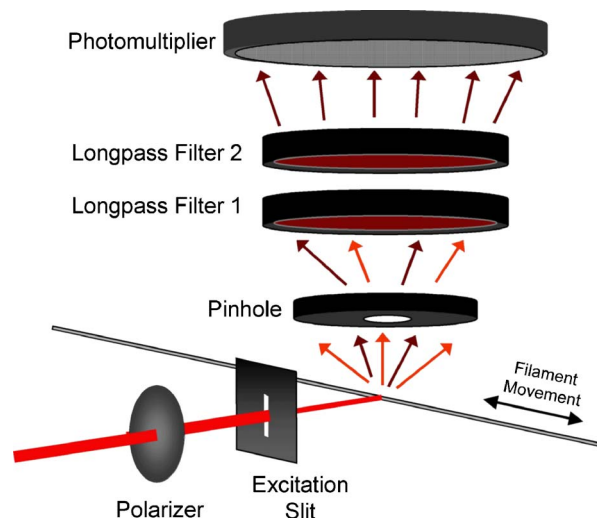

Fig. 2 Optical path of virus detection system. Using a 638-nm laser excitation source, detection of filament fluorescence is possible using the appropriate emission filters. Exposure area on the filament is reduced by an excitation slit.

Table 2 Incubation parameters for all experiments.

Experiment	Virus time (min)	Wash (min)	Detecting Ab incubation (min)	Final wash (min)
Basic detection	30	3	10	5
Laser effects	30	3	5	5
Fast detection	1	0.25	1	0.25
Virus sensitivity	1,10,40	1	5	1
Reposition to detecting Ab chamber	30	3	0.5, 1, 2	5
Reposition to virus chamber	1,5,10	1	5	1

peak values with average anti-E values to determine statistical significance. P values less than 0.05 signified positive virus detection.

Basic system tests were performed to show the effectiveness of the optical system and to determine some standard parameters that helped optimize signal to noise (Table 2). These tests were designed to determine FARA SNR and to determine if laser exposure significantly bleached the label on the detecting antibody. Preliminary observations using the laser at full power (25 mW) showed that laser exposure may decrease fluorescence on repeated scans. To show that this effect was minimized with a less powerful laser beam, multiple laser scans of two filaments were performed after a typical virus detection experiment. One set of scans used the full power 25-mW laser, while the other used a reduced power of approximately 5 mW. The change in SNR with each scan was then calculated. Incubation parameters for these system tests are summarized in Table 2.

Once basic parameters were established, incubation times were shortened to determine the shortest assay time that resulted in positive virus detection. Virus and detecting antibody incubation times were shortened to one minute, and wash times were shortened to fifteen seconds. When this shortened assay time was established, experiments were performed to determine the limit of sensitivity of this technique and the minimum assay times required to detect lower virus concentrations. Virus concentrations from 3.3×10^7 to 3.3×10^{10} were used for these experiments. Virus incubation time was increased until detection was achieved. A summary of these parameters is shown in Table 2.

Important aspects of this assay design are the online detection of fluorescence associated with virus capture and the continuous control of filament position. This combination suggests that feedback from the detector signal could be used to direct subsequent filament motion. In this assay, there are two methods to increase the fluorescence signal associated with virus capture. One approach is to increase the number of detecting antibodies associated with each virus-antibody complex on the filament. Assuming that the initial residence time within the detecting antibody chamber is initially suboptimal, increasing this time should increase the signal. In the first experimental design to evaluate this capability, a filament containing three capture antibody regions and one negative control region was incubated for 30 sec in the detecting anti-body chamber and scanned. The capture-antibody region of this filament was repositioned in the detecting antibody chamber for an additional 30 sec and rescanned. This cycle was repeated four times.

The second approach to increase signal is to increase the number of antibody-virus complexes associated with the filament. This can potentially be done by increasing the residence time in the virus chamber. Therefore, in the second experimental test, the filament was repositioned back to the virus chamber. In this test, the first cycle of each experiment used a one-minute virus incubation that yielded only a weak signal. Following this initial measurement, the capture antibody region of the filament was repositioned within the virus chamber for additional incubation. After each additional virus incubation, processing within chambers 3, 4, and 5 was repeated. The filament was cycled through this process three times to show the capability of using on-line detection and filament motion to enhance the fluorescence signal. Table 2 summarizes incubation parameters for both repositioning experiments.

2.6 Results

As described later, repositioning the regions of the filament containing the capture antibodies through the reaction chambers and detector in an effort to increase the signal was an important aspect of many experiments. One concern with this approach is the bleaching effect of laser illumination on the fluorescent molecules and on the antigen-antibody interactions. Therefore, we first verified that consecutive fluorescence measurements produced similar intensities. Effects of laser illumination were investigated by taking multiple scans of two filaments following two virus detection experiments. Each filament was prepared with three anti-M13 regions and processed as summarized in Table 2. As Fig. 3 illustrates, full-power laser exposure decreased the observed signal during repeated scanning. After five successive scans, the signal was reduced to ~8% of its initial value (black bars). We reduced the laser power to determine if this would prevent the drop in signal intensity for subsequent scans. A polarizer was used to reduce laser power from its full strength of 25 mW to approximately 5 mW. To further reduce laser exposure of the filament, the filament scanning speed was increased to 4 cm/sec and an excitation slit was placed in front of the
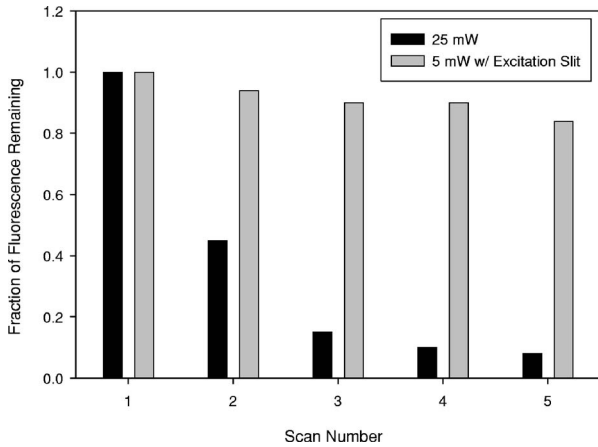
Fig. 3 Effects of laser power on scan repeatability. Repeated laser scans of virus detection filaments result in a significant signal drop for filaments using full laser power (black bars) but not with reduced laser power (gray bars).

laser. As shown by the gray bars in Fig. 3, a reduced laser power had a much lower effect. After five successive scans, fluorescence was still above 80% of the initial value. All subsequent results were obtained using the polarizer and excitation slit.

Figure 4 shows that regions of the filament containing the capture antibody (anti-M13) produced strong fluorescence signals. In these experiments each ~3-cm length of the filament included one negative control anti-E region and three anti-M13 regions. After processing through the five chambers, strong fluorescence signal (SNR 51 ± 4.5) was observed in regions of the filament containing immobilized anti-M13 capture antibody, indicating successful virus detection. The fluorescence observed in the region containing immobilized anti-E capture antibody is indistinguishable from the background. The lack of fluorescence in the anti-E region of the filament indicates that, as expected, antigen/antibody binding
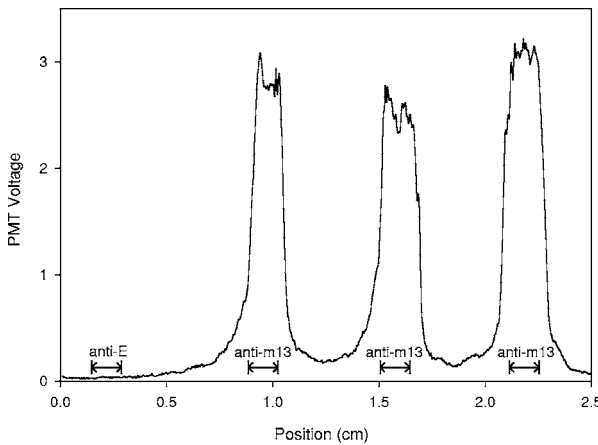

Fig. 4 Representative filament scan showing photomultiplier output as a function of filament position. Laser scanning of the filament detects virus in all three capture antibody regions (anti-M13) with a SNR of approximately 51 ± 4.5. Negative control antibody region (anti-E) is not distinguishable from background. Arrows indicate the location of each immobilized antibody region along the filament.
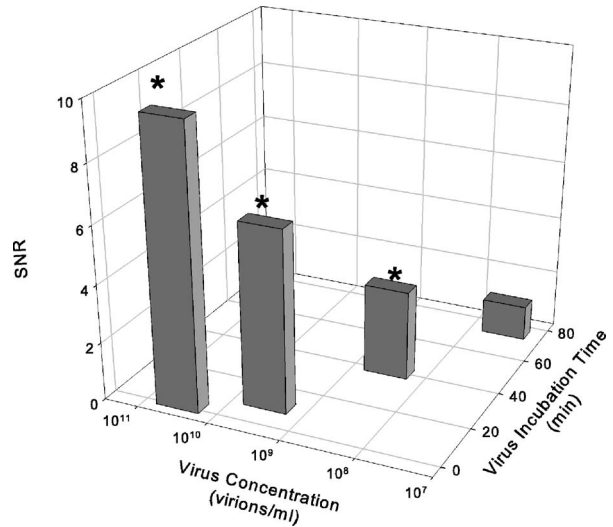

Fig. 5 Virus incubation times required to detect different virus concentrations. A one-minute virus incubation detected 3.3×10^{10} virions/ml with a SNR of nearly 10. Concentrations below 3.3×10^{8} virions/ml were not detectable with a 75-min virus incubation time. Asterisks indicate that a difference in fluorescence signal between capture antibody regions and regions without antibodies is statistically significant ($p<0.05$).

is a highly specific process and that no virus was attached to this region. Scanning a filament with both the integrated detector and using the previous method of a flatbed microarray scanner,[13] we found that SNR increased by nearly a factor of 5.

In this system, higher virus concentrations could be detected with shorter virus incubation times. Figure 5 shows the virus incubation time required to detect virus of different concentrations along with the SNR achieved in each experiment. Detection of 3.3×10^{8} virions/ml was achieved in 40 min with a SNR of more than 3. Raising the virus concentration to 3.3×10^{9} virions/ml reduced the required virus incubation time to 10 min, while raising the SNR to more than 6. Concentrations of 3.3×10^{10} virions/ml, the highest concentration tested, reduced the required time even further to only 1 min and resulted in a high SNR of almost 10. All other reaction parameters remained constant for these experiments (Table 2), so the total assay times for these trials ranged from 41.5 min for the lowest concentration to only 2.5 min for the highest concentration. Since filament blocking can be performed ahead of time, blocking times were not included in these estimates.

Online detection and control of filament position are unique aspects of FARA. In this approach, a weak signal could potentially be amplified by reprocessing the immobilized capture antibody regions through the reaction chambers. This aspect could be very important for a new antibody/ antigen pair, for which optimal incubation times are not yet known, or for rapid detection applications in which time is critical. In this approach, a rapid detection protocol might be used to detect a high virus titer, but if the initial screen is negative, then a higher-sensitivity, slower detection protocol could be used. As an initial test of this strategy, experiments were performed to test the effects on the fluorescence of re-
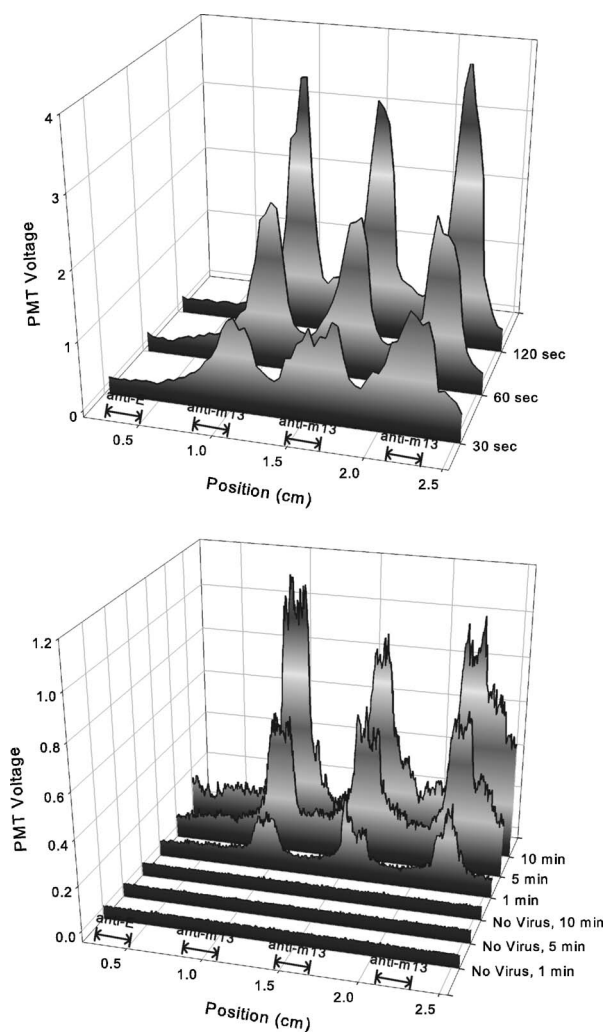
Fig. 6 Effects of reprocessing on fluorescence. Signal increases as the capture antibody region of the filament is cycled back to the detecting antibody chamber (top) or the virus chamber (bottom) for additional incubation. Arrows indicate regions of immobilized antibodies. The lower sampling rate in the top panel resulted in a smoother curve. Virus concentration was 3.3×10^{10} virions/ml.

positioning the capture antibody regions of the filament within the detecting antibody chamber. The top panel of Fig. 6 shows the increase in signal after the filament was cycled through the detecting antibody chamber three times for additional incubation. In this assay, signal strength increases by almost a factor of 4 as the filament region containing the capture antibodies is reincubated within the virus test solution.

Next, a second test of this strategy was performed by repositioning the capture regions within the virus chamber for increasing incubation times. In these experiments, a short initial virus incubation time was used for virus detection, so that fluorescence intensity was initially low. After the initial processing was performed and the filament scanned, the filament was repositioned within the virus chamber for an additional incubation, followed by the standard processing steps in the subsequent chambers. The bottom of Fig. 6 shows the increases in signal for cumulative incubation times of 1, 5, and 10 min.
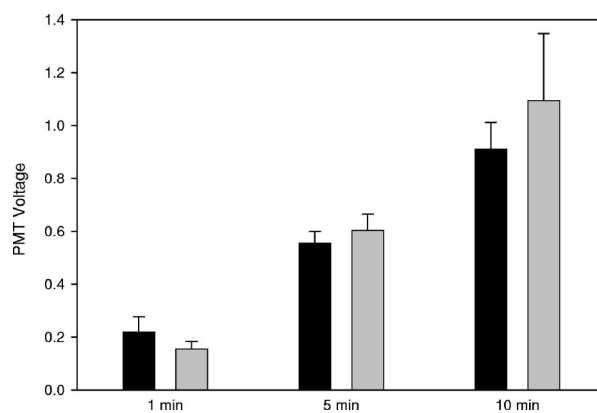

Fig. 7 Comparison of multiple short virus incubations (black bars) to one long virus incubation (gray bars). Virus cumulative incubation times of 1, 5, or 10 min resulted in similar fluorescence for a single filament exposed multiple times or for separate filaments each exposed for the same cumulative time indicated. Virus concentration was 3.3×10^{10} virions/ml.

The filament used for this experiment contained an anti-E negative control region adjacent to three anti-M13 regions. Fluorescence increases approximately 4 to 5 fold for the anti-M13 regions from cycle 1 to 3, but there is almost no change in the control antibody region. In addition, a negative control experiment was performed to ensure that increases in fluorescence were a result of specific antigen/antibody interactions. This experiment used an equivalent filament and experimental parameters, but no virus was used for this assay. The lower panel of Fig. 6 ("no virus" traces) shows that after three cycles through the incubation chambers, fluorescence does not increase above background.

As a final test of the filament repositioning strategy, we compared the signal intensities obtained with a single pass through the reaction chambers to the intensities obtained with filaments cycled through three successive processing cycles. As Fig. 7 indicates, the reincubation strategy produced signal intensities very similar to intensities of filaments with continuous incubation times when cumulative virus incubation times were matched. This indicates that filament motion and additional processing steps do not reduce the observed signal. Furthermore, it suggests that by using this system, flexible adaptive processing strategies utilizing repositioning of the filament after fluorescence measurements can be developed.

3 Discussion

Previous work on FARA has shown the potential of filament-based virus detection.[13] High levels of sensitivity and specificity have been shown, along with automated processing. However, automation was limited to filament processing, requiring filaments to be removed for fluorescence scanning on a microarray scanner. The focus of the present work is the design and development of a fluorescence-based on-line detector that is integrated with the existing system of microreaction chambers (Fig. 1). On-line fluorescence detection allows automation of the entire virus detection process. Figure 4 shows typical virus detection results using FARA's integrated optical detection system. The distinct peaks in the anti-M13 regions indicate that M13 virus bound to the regions in which

capture antibody was coupled to the filament. Captured virus subsequently bound a fluorescently labeled detecting antibody as the filament moved through the detecting-antibody chamber. Specificity of virus detection is demonstrated by the lack of any detectable peak in the negative control anti-E region. Average SNR for this experiment was more than 50, which exceeded the values previously reported for FARA, even though the assay time was shortened from approximately 100 min to approximately 50 min.

Much of the increase in SNR and decrease in assay time can be attributed to the optical flexibility of FARA's integrated detector. This detector allows any single filter or combination of filters to be used in the emission path. The ability to customize and adjust the emission filters is a major factor in the high SNR. Previously, detection was achieved using a dual laser microarray scanner with set emission filters that were not optimal for this application. Emission bandpass filters for the microarray scanner had a very broad bandwidth, so numerous fluorescent dyes could be used. However, these broad emission filters also passed a significant degree of background fluorescence, which limited SNR. We are currently modifying the design to eliminate most of the specular reflectance by mounting the PMTs at a 45-deg angle from vertical, so that the line of reflection is not captured. This should help to further improve SNR achievable with this approach.

The on-line detection of fluorescence combined with filament movement control give FARA the unique advantage of rapid initial virus detection testing for high concentration of virus, followed by a high sensitivity test for low concentrations of virus. As shown in Fig. 6, this feature can be used to optimize and increase signal. Fluorescence from the capture regions increases significantly after each additional incubation in both the virus chamber and the detecting antibody chamber. Importantly, multiple repositioning does not appear to reduce the signal intensity achieved with a single pass (Fig. 7). A region of interest on the filament can be processed and reprocessed until the fluorescence signal reaches a predetermined level. For example, the virus detection program could continue to cycle the filament back through the reaction chambers until the signal reached this level or until total assay time reached a preset limit. This could be very useful for less well-characterized antigen/antibody pairs, for which optimal incubation times are not known. On-line fluorescence detection could also be a very valuable tool for guiding further testing. Multiple groups of antibody regions, each corresponding to a different test, could be immobilized along a long filament. The results from one group could determine which group is tested next. In this manner, a sample could be probed for many antigens in the order which best preserves the sample and provides the maximum information about the unknown sample. A manuscript describing a test of this strategy is being prepared for publication.[14]

Laser power requirements for filament-based virus detection using FARA was not known, so a 25-mW diode laser was a cost efficient way to ensure that ample power was available. The initial laser detection system appeared to decrease the observable signal intensities seen in subsequent readings. Initial experiments utilized the excitation laser at its full strength of 25 mW, but qualitative observations indicated that repeated laser exposure at this intensity reduced fluorescence not only through bleaching effects, but also possibly through an unidentified interruption of the antibody-antigen interaction. Experiments exposing the filament to the laser as it exited either the virus chamber (data not shown) or the final wash chamber helped to distinguish between bleaching effects and the effects on antibody-antigen interactions. In both experimental designs, repeated scans reduced the signal intensity. Exposure of the filament to the laser immediately after the virus chamber reduced the SNR by a factor of 4, indicating the antibody-antigen interactions were being disrupted, since no labeled antibody was present at the point in the assay. When the filament was exposed to the laser following the final wash, SNR was also reduced by approximately a factor of 4, indicating that bleaching of the fluorophore occurred. Based on these observations, we conclude that laser interactions with both the fluorophore and the antibody-antigen binding partners contribute to the decline in signal intensity. Beaching effects are well known; however, there appear to be few reports or studies directed at the effects of antibody-antigen binding.

Since laser power appeared to be important, we also estimated the light exposure produced under the conditions of these experiments. The calculated laser exposure for each capture region of the filament using full laser power was approximately 1.13 mJ during scanning. This calculation was based on the laser power (25 mW), region width (1.5 mm), the initial slow scan speed of 0.5 cm/s, and the width of the filament relative to the laser beam. The antigen-antibody interaction is typically made of several noncovalent interactions such as hydrogen bonding, dipole-dipole interactions, hydrophobic interactions, van der Waals forces, and sometimes electrostatic interactions. The strength of the overall interaction is a summation of these individual interactions with electrostatic interactions and hydrogen bonding being the strongest bonds at 670 and 20 kJ/mol, respectively. The strength of the antibody-antigen bond is strongly dependent on the proximity of the contact areas between the antibody paratope and the binding epitope on the antigen. Since every interaction is different, the total energy of such interactions may range from the tens to hundreds of kJ/mol. Even if it is assumed that 100% of the antibody from the spotting solution adsorbs to the filament and binds virus after the initial washing and blocking step, there is still ample laser energy to disrupt all virus-antibody interactions if all laser energy were completely absorbed by the surface molecules. However, an accurate calculation of this energy is difficult to obtain due to two major unknowns. It is unknown how much antibody from the initial spotting solution binds to the filament and how much remains active. In addition, the energy transferred from the laser beam to surface antibodies on the filament is also difficult to calculate. Even though the laser exposure is easy to estimate, the amount of absorbed laser light is still uncertain. Most of the absorption of laser light is by the filament itself, so it remains unclear how much of this energy is being transferred to the antibodies and antigens on the filament. Since the laser is at a wavelength (638 nm) that is not highly absorbed by proteins, the antibodies themselves should not absorb a significant amount of energy. Nevertheless, laser exposure at full power was shown to disrupt virus binding. Weakened interactions between virus and antibody allowed the virus to be washed off when the capture regions were sent back through the system for additional incubations. To limit these effects, a polar-

izer was placed in front of the laser and adjusted so that the laser output was reduced to 5 mW. To reduce exposure even further, the filament scanning speed was increased to 4 cm/sec and an exposure slit was built to reduce the area of the filament that was illuminated by 50%. These modifications reduced filament exposure by a factor of 100 to approximately 0.014 mJ, and laser effects were minimized.

In summary, the addition of an online optical fluorescence detector increases the sensitivity of FARA and provides additional processing flexibility that makes adaptive detection feasible.

Acknowledgments

References

1. S. S. Iqbal, M. W. Mayo, J. G. Bruno, B. V. Bronk, C. A. Batt, and J. P. Chambers, "A review of molecular recognition technologies for detection of biological threat agents," *Biosens. Bioelectron.* **15**(11-12), 549–578 (2000).

2. L. F. Peruski, Jr. and A. H. Peruski, "Rapid diagnostic assays in the genomic biology era: detection and identification of infectious disease and biological weapon agents," *BioTechniques* **35**(4), 840–846 (2003).

3. P. E. Andreotti, G. V. Ludwig, A. H. Peruski, J. J. Tuite, S. S. Morse, and L. F. Peruski, Jr., "Immunoassay of infectious agents," *BioTechniques* **35**(4), 850–859 (2003).

4. M. D. Marazuela and M. C. Moreno-Bondi, "Fiber-optic biosensors—an overview," *Anal. Bioanal. Chem.* **372**(5-6), 664–682 (2002).

5. P. D'Orazio, "Biosensors in clinical chemistry," *Clin. Chim. Acta* **334**(1-2), 41–69 (2003).

6. D. R. Baselt, G. U. Lee, K. M. Hansen, L. A. Chrisey, and R. J. Colton, "A high-sensitivity micromachined biosensor," *Proc. IEEE* **85**(4), 672–680 (1997).

7. Z. Mubammad-Tahir and E. C. Alocilja, "A conductometric biosensor for biosecurity," *Biosens. Bioelectron.* **18**(5-6), 813–819 (2003).

8. N. J. Ronkainen-Matsuno J. H. Thomas, H. B. Halsall, and W. R. Heinemann, "Electrochemical immunoassay moving into the fast lane," *TrAC, Trends Anal. Chem.* **21**(4), 213–225 (2002).

9. A. Balasubramanian, B. Bhuva, R. Mernaugh, and F. R. Haselton, "Si-based sensor for virus detection," *IEEE Sens. J.* **5**(3), 340–344 (2005).

10. T. E. Plowman, J. D. Durstchi, H. K. Wang, D. A. Christensen, J. N. Herron, and W. M. Reichert, "Multiple-analyte fluoroimmunoassay using an integrated optical waveguide sensor," *Anal. Chem.* **71**(19), 4344–4352 (1999).

11. C. A. Rowe, L. M. Tender, M. J. Feldstein, J. P. Golden, S. B. Scruggs, B. D. MacCraith, J. J. Cras, and F. S. Ligler, "Array biosensor for simultaneous identification of bacterial, viral, and protein analytes," *Anal. Chem.* **71**(17), 3846–3852 (1999).

12. F. S. Ligler, C. R. Taitt, L. C. Shriver-Lake, K. E. Sapsford, Y. Shubin, and J. P. Golden, "Array biosensor for detection of toxins," *Anal. Bioanal. Chem.* **377**(3), 469–477 (2003).

13. G. P. Stone, R. Mernaugh, and F. R. Haselton, "Virus detection using filament-coupled antibodies," *Biotechnol. Bioeng.* **91**(6), 699–706 (2005).

14. G. P. Stone, T. S. Dermody, J. D. Wetzel, P. K. Russ, and F. R. Haselton, "Autonomous Reovirus strain classification using filament-coupled antibodies" (unpublished).